

# Analysis of a Multigrid Method for a Transport Equation by Numerical Fourier Analysis <sup>1</sup>

S. OLIVEIRA

Department of Computer Science  
Texas A&M University, College Station, TX 77843-3112.  
suelv@cs.tamu.edu

ABSTRACT. In this paper, we perform Fourier analysis for a multigrid method with two-cell  $\mu$ -line relaxation for solving isotropic transport equations. Our numerical results show that the Fourier analysis prediction for convergence rates is more accurate than that previously found by matrix analysis.

KEYWORDS. Fourier analysis, multigrid, transport equations.

## 1. INTRODUCTION

In this paper, we develop a Fourier analysis for a multigrid method which solves the isotropic transport equation in slab geometry given by

$$(1) \quad \mu \frac{\partial \psi}{\partial x}(x, \mu) + \sigma_t \psi(x, \mu) = \frac{1}{2} \sigma_s \int_{-1}^1 \psi(x, \mu') d\mu' + q(x, \mu), \quad x \in (0, 1), \quad \mu \in [-1, 1],$$

where  $\psi(x, \mu)$  represents the flux of particles at position  $x$  traveling at an angle  $\theta = \arccos(\mu)$  from the  $x$ -axis,  $\sigma_t$  is the macroscopic total cross section,  $q(x, \mu)$  is an external source. In what follows, we shall omit the external source term  $q$  for simplicity. The boundary conditions for equation (1) are given by

$$(2) \quad \psi(0, \mu) = g_0(\mu), \quad \psi(1, -\mu) = g_1(\mu), \quad \mu \in (0, 1),$$

which prescribe the flux of particles entering the slab.

The transport problem given by equations (1) and (2) arises in many applications, such as nuclear reactor design, radiative transfer, and gas kinetics. Various numerical methods have been developed for the transport problem (1, 2), such as diffusion synthetic acceleration scheme (DSA) [1], and multigrid methods [3, 4, 5, 9]. In our work, we use the Modified Linear Discontinuous (MLD) method for the discretization and a spatial multigrid method for solving the resulting system of equations. In particular, the multigrid method we consider here is based on a so-called two-cell  $\mu$ -line relaxation, which was developed in [4]. The matrix analysis for the transport equation with isotropic scattering was also presented there. It was shown that for pure scattering ( $\sigma_s = \sigma_t$ ), the convergence factor for the multigrid method is of order  $O((\frac{1}{\sigma_t h})^2)$  when  $\sigma_t h \gg 1$  and  $O((\sigma_t h)^3)$  when  $\sigma_t h \ll 1$ . In this paper, we present the Fourier analysis for the multigrid algorithm. Our results show that the Fourier analysis predictions for convergence rates are more accurate than that from the matrix analysis in [4]. While the Fourier Analysis results obtained ultimately required some numerical computation, the amount of computation needed was far less than what is needed to implement the multigrid algorithm.

An outline of the remainder of this paper is as follows. In Section 2, we briefly describe the center-edge discretization and derive the corresponding equations in edge-edge notation.

---

<sup>1</sup>This research was partially supported by NSF grant ASC 9528912 and a Texas A&M University Interdisciplinary Research Initiative Award.

In Section 3, we present the Fourier analysis for a two-level multigrid scheme. In Section 4, we show results for the of convergence rates obtained from Fourier Analysis, and compare them against the actual convergence rates in [4].

## 2. DISCRETIZATION

We discretize equation (1) by applying  $P_{N-1}$  approximations with respect to angle variable  $\mu$  and then MLD scheme with respect to spatial variable  $x$ ; see [10] for details. For slab geometry, the  $P_{N-1}$  discretization is equivalent to collocating at Gauss quadrature points  $\{\mu_i\}_{i=1}^N$  with weights  $\{w_i\}_{i=1}^N$ . We assume that  $N$ , the degree of Gauss quadrature, is even and  $N = 2n$ . Thus,  $\mu_k = -\mu_{k+n} > 0$  and  $w_k = w_{k+n}$ ,  $k = 1, \dots, n$ . There are two notations for the MLD scheme: center-edge notation and edge-edge notation. Let us consider spatial grid  $0 = x_{\frac{1}{2}} < x_{\frac{3}{2}} < \dots < x_{m+\frac{1}{2}} = 1$ . In the center-edge notation, we denote by  $x_{i+1/2}$  the cell edges and by  $x_i = (x_{i-1/2} + x_{i+1/2})/2$  the cell center. Let  $\psi_{i-\frac{1}{2},j}^- = \psi(x_{i-\frac{1}{2}}, -\mu_j)$ ,  $\psi_{i,j}^+ = \psi(x_i, \mu_j)$ ,  $\psi_{i,j}^- = \psi(x_i, -\mu_j)$ , and  $\psi_{i+\frac{1}{2},j}^+ = \psi(x_{i+\frac{1}{2}}, \mu_j)$ . Using vector notation  $\underline{\psi}_i^\pm = [\psi_i^\pm(x_i, \mu_1), \psi_i^\pm(x_i, \mu_2), \dots, \psi_i^\pm(x_i, \mu_n)]^T$ , which represent flux at spatial point  $x_i$ , angular position  $\mu_j$  in positive (+) and negative (-) directions, respectively. Then the discrete equations can be written in center-edge notation as

$$\begin{aligned} (3) \quad & B_i(\underline{\psi}_{i+\frac{1}{2}}^+ - \underline{\psi}_{i-\frac{1}{2}}^+) + \underline{\psi}_i^+ = R(\underline{\psi}_i^+ + \underline{\psi}_i^-), \\ (4) \quad & 2B_i(\underline{\psi}_{i+\frac{1}{2}}^+ - \underline{\psi}_i^+) + \underline{\psi}_{i+\frac{1}{2}}^+ = R(\underline{\psi}_{i+\frac{1}{2}}^+ + 2\underline{\psi}_i^- - \underline{\psi}_{i-\frac{1}{2}}^-), \\ (5) \quad & B_i(\underline{\psi}_{i-\frac{1}{2}}^- - \underline{\psi}_{i+\frac{1}{2}}^-) + \underline{\psi}_i^- = R(\underline{\psi}_i^+ + \underline{\psi}_i^-), \\ (6) \quad & 2B_i(\underline{\psi}_{i-\frac{1}{2}}^- - \underline{\psi}_i^-) + \underline{\psi}_{i-\frac{1}{2}}^- = R(\underline{\psi}_{i-\frac{1}{2}}^- + 2\underline{\psi}_{i-\frac{1}{2}}^- + 2\underline{\psi}_i^+ - \underline{\psi}_{i+\frac{1}{2}}^+), \\ & i = 1, \dots, m, \end{aligned}$$

where  $B_i = \text{diag}(\frac{\mu_1}{\sigma_i h_i}, \dots, \frac{\mu_n}{\sigma_i h_i})$ ,  $R = \underline{\mathbf{1}}\underline{\mathbf{w}}^T$ ; see [4] for a complete description. In the edge-edge notation, we denote by  $x_{i,l}$  and  $x_{i,r}$  the left and right edges of cell  $i$ , respectively. Let

$$(7) \quad \underline{\psi}_{i,l}^+ = 2\underline{\psi}_i^+ - \underline{\psi}_{i+\frac{1}{2}}^+, \quad \underline{\psi}_{i,r}^+ = \underline{\psi}_{i+\frac{1}{2}}^+, \quad \underline{\psi}_{i,l}^- = \underline{\psi}_{i-\frac{1}{2}}^-, \quad \underline{\psi}_{i,r}^- = 2\underline{\psi}_i^- - \underline{\psi}_{i-\frac{1}{2}}^-.$$

Since the flux within cell  $i$  is linear,  $\underline{\psi}_{i,l}^\pm$  and  $\underline{\psi}_{i,r}^\pm$  represent the flux at the left and right sides of the cell, respectively. We can reformulate equations (3)–(6) in the edge-edge notation as

$$\begin{aligned} (8) \quad & B_i(\underline{\psi}_{i,l}^+ + \underline{\psi}_{i,r}^+) - 2B_i\underline{\psi}_{i-1,r}^+ + \underline{\psi}_{i,l}^+ = R\underline{\psi}_{i,l}^+, \\ (9) \quad & B_i(\underline{\psi}_{i,r}^+ - \underline{\psi}_{i,l}^+) + \underline{\psi}_{i,r}^+ = R\underline{\psi}_{i,r}^+, \\ (10) \quad & B_i(\underline{\psi}_{i,l}^- + \underline{\psi}_{i,r}^-) - 2B_i\underline{\psi}_{i+1,l}^- + \underline{\psi}_{i,r}^- = R\underline{\psi}_{i,r}^-, \\ (11) \quad & B_i(\underline{\psi}_{i,l}^- - \underline{\psi}_{i,r}^-) + \underline{\psi}_{i,l}^- = R\underline{\psi}_{i,l}^-, \\ & i = 1, \dots, m. \end{aligned}$$

Throughout our Fourier analysis, we will use the edge-edge notation unless otherwise stated.

## 3. ANALYSIS FOR A TWO-LEVEL ALGORITHM

Equations (8)–(11) can be solved by multigrid methods [2, 4]. In this section, we will show the Fourier analysis method for a two-grid multigrid algorithm, where the two-cell  $\mu$ -line relaxation (Jacobi or red-black Gauss-Seidel) is used in presmoothing and postsmoothing stages [4]. By two-cell  $\mu$ -line relaxation, we mean that using boundary values of two adjacent

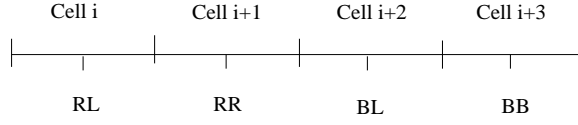


FIGURE 1. Group of cells for Fourier analysis.

cells, one solves for all other interior points in the two cells simultaneously. For introduction to Fourier analysis for multigrid methods, the reader is referred to [11].

For the red-black Gauss-Seidel relaxation, we consider a group of four cells. We define two black cells (BL - black left and BR - black right) and two red cells (RL - red left and RR - red right) as indicated in Figure 1.

Let

$$\begin{aligned} \underline{\psi}(x, \mu) &= \\ & [\underline{\psi}_{i,l}(x, \mu) \ \underline{\psi}_{i,r}(x, \mu) \ \underline{\psi}_{i+1,l}(x, \mu) \ \underline{\psi}_{i+1,r}(x, \mu) \ \underline{\psi}_{i+2,l}(x, \mu) \ \underline{\psi}_{i+2,r}(x, \mu) \ \underline{\psi}_{i+3,l}(x, \mu) \ \underline{\psi}_{i+3,r}(x, \mu)]^T, \\ \underline{\psi}_f(\lambda, \mu) &= \\ & [\underline{\psi}_l^{RL}(\lambda, \mu) \ \underline{\psi}_r^{RL}(\lambda, \mu) \ \underline{\psi}_l^{RR}(\lambda, \mu) \ \underline{\psi}_r^{RR}(\lambda, \mu) \ \underline{\psi}_l^{BL}(\lambda, \mu) \ \underline{\psi}_r^{BL}(\lambda, \mu) \ \underline{\psi}_l^{BR}(\lambda, \mu) \ \underline{\psi}_r^{BR}(\lambda, \mu)]^T, \end{aligned}$$

where  $\underline{\psi}_f(\lambda, \mu)$  is the Fourier coefficient of  $\underline{\psi}(x, \mu)$  with respect to Fourier mode  $e^{i\lambda x}$ , namely,

$$(12) \quad \underline{\psi}(x, \mu) = e^{i\lambda x} \underline{\psi}_f(\lambda, \mu),$$

for one Fourier mode. For all the modes, for  $P$  groups of 4 cells with periodic boundaries, we can write  $\underline{\psi}(x, \mu) = \sum_{k=0}^{P-1} \underline{\psi}_f(\lambda_k, \mu) e^{i\lambda_k x}$ , where  $\lambda_k = \frac{\pi k}{2hP}$ ,  $k = 0, 1, \dots, P-1$ .

To perform Fourier analysis for the multigrid scheme, we denote the relaxation step by  $A\underline{\psi}^{l+1} = B\underline{\psi}^l$ , where matrices  $A$  and  $B$  are derived by substituting (12) into equations (8–11) for the  $\mu$ -line two-cell relaxation (Jacobi or red-black Gauss-Seidel). This implies that the matrices  $A$  and  $B$  depend on  $\lambda$ . It is noted that the MLD relaxation will always be represented by four equations for each cell with two equations for each direction. Thus, for the the red-black Gauss-Seidel relaxation, the number of equations is  $8 \times$  (number of directions). We update all the red cells before any of the black cells. Consequently, when we write the MLD equations for red cells in the Fourier analysis, variables corresponding to black cells are assumed to be at iteration level  $l$  instead of  $l+1$ . But when we write the MLD equations for black cells, variables corresponding to both red and black cells are at iteration level  $l+1$  (so they do not contribute terms to the right-hand side of the equations). The Fourier analysis for the Jacobi relaxation is done similarly — in fact, its analysis is simpler than the red-black Gauss-Seidel case. The main difference is that we need to consider only one kind of cell pair and when referencing cell pairs other than the one we are writing equations for, the variables are assumed to be at iteration level  $l$ . To reflect the multigrid level, we write  $A^h \underline{\psi}^{l+1} = B^h \underline{\psi}^l$  for the fine grid and  $A^{2h} \underline{\psi}^{l+1} = B^{2h} \underline{\psi}^l$  for the coarse grid, where  $h$  is the length of a cell at the fine grid. Let  $I_{2h}^h$  and  $J_h^{2h}$  be the interpolation and restriction operators in the edge-edge notation, respectively. Then, the Fourier analysis for two-level mutigrid  $V(1, 1)$ -cycle can be carried out by the following steps:

- (1) Relaxation on the fine grid:  $\underline{\psi}^{l+\frac{1}{3}} = (A^h)^{-1} B^h \underline{\psi}^l$ .
- (2) Calculation of the residual on the fine grid:  $\underline{r}^h = B^h ((A^h)^{-1} B^h - I) \underline{\psi}^{l+\frac{1}{3}}$ .
- (3) Transfer of the residual to the coarse grid:  $\underline{f}^{2h} = I_{2h}^{2h} \underline{r}^h = I_{2h}^{2h} B^h ((A^h)^{-1} B^h - I) \underline{\psi}^l$ .
- (4) Calculation of the error on the coarse grid:  $\underline{e}^{2h} = (A^{2h} - B^{2h})^{-1} \underline{f}^{2h}$ .
- (5) Correction to the solution:  $\underline{\psi}^{l+\frac{2}{3}} = \underline{\psi}^{l+\frac{1}{3}} + I_{2h}^h \underline{e}^{2h}$ .

(6) Relaxation on the fine grid:  $\underline{\psi}^{l+1} = (A^h)^{-1} B^h \underline{\psi}^{l+\frac{2}{3}}$ .

It is easy to show that the convergence rate for the two-level multigrid  $V(1,1)$ -cycle is given by the spectral radius of the following matrix:

$$(13) \quad Z = (A^h)^{-1} B^h [(A^h)^{-1} B^h + I_{2h}^h (A^{2h} - B^{2h})^{-1} I_h^{2h} B^h ((A^h)^{-1} B^h - I)],$$

which depends on  $\lambda$ . Thus, the convergence factor for the Fourier analysis is the maximum spectral radius of  $Z$  over the set  $\lambda_k = \frac{\pi k}{2hP}$ ,  $k = 0, \dots, P-1$ .

In the remainder of this section, we show the derivation of matrix  $Z$  for both red-black Gauss-Seidel and Jacobi relaxations.

1. Equations on the fine grid. These equations generate matrices  $A^h$  and  $B^h$  used in Step 1. When the Fourier modes are substituted in equations (8–11) for the four cells, red-black relaxation can be written as

$$(14) \quad \begin{bmatrix} F & U & 0 & 0 \\ L & F & 0 & 0 \\ 0 & L & F & U \\ Ue^{i\lambda H} & 0 & L & F \end{bmatrix} \underline{\psi}^{l+1} = \begin{bmatrix} 0 & 0 & 0 & -Le^{-i\lambda H} \\ 0 & 0 & -U & 0 \\ 0 & 0 & 0 & 0 \\ 0 & 0 & 0 & 0 \end{bmatrix} \underline{\psi}^l,$$

where

$$H = 4h, \quad F = \sigma_i h \begin{bmatrix} I + B_i - R & -R & -B_i & 0 \\ -R & I + B_i - R & 0 & B_i \\ B_i & 0 & I + B_i - R & -R \\ 0 & -B_i & -R & I + B_i - R \end{bmatrix},$$

$$U = \sigma_i h \begin{bmatrix} 0 & 0 & 0 & 0 \\ 0 & 0 & 0 & 0 \\ -2B_i & 0 & 0 & 0 \\ 0 & 0 & 0 & 0 \end{bmatrix}, \quad L = \sigma_i h \begin{bmatrix} 0 & 0 & 0 & 0 \\ 0 & 0 & 0 & -2B_i \\ 0 & 0 & 0 & 0 \\ 0 & 0 & 0 & 0 \end{bmatrix}.$$

The order of variables for this matrix is  $\underline{\psi} = (\underline{\psi}^{RL}, \underline{\psi}^{RR}, \underline{\psi}^{BL}, \underline{\psi}^{BR})$ , where

$$\underline{\psi}^{RL} = (\underline{\psi}_l^{-RL}, \underline{\psi}_l^{+RL}, \underline{\psi}_r^{-RL}, \underline{\psi}_r^{+RL}), \quad \underline{\psi}^{RR} = (\underline{\psi}_l^{-RR}, \underline{\psi}_l^{+RR}, \underline{\psi}_r^{-RR}, \underline{\psi}_r^{+RR}),$$

$$\underline{\psi}^{BL} = (\underline{\psi}_l^{-BL}, \underline{\psi}_l^{+BL}, \underline{\psi}_r^{-BL}, \underline{\psi}_r^{+BL}), \quad \underline{\psi}^{BR} = (\underline{\psi}_l^{-BR}, \underline{\psi}_l^{+BR}, \underline{\psi}_r^{-BR}, \underline{\psi}_r^{+BR}).$$

For Jacobi relaxation, considering  $F$ ,  $L$  and  $U$  as before and letting  $H = 2h$ , we have

$$(15) \quad \begin{bmatrix} F & U \\ L & F \end{bmatrix} \underline{\psi}^{l+1} = \begin{bmatrix} 0 & -Le^{-i\lambda H} \\ -Ue^{i\lambda H} & 0 \end{bmatrix} \underline{\psi}^l.$$

2. Equations on the coarse grid. These equations will generate the matrix  $A^{2h} - B^{2h}$  for Step 4. The equations on this level are assumed to be solved exactly. Since coarsening the grid halves the number of points, on the coarse grid we will have two cells in the Fourier analysis for red-black Gauss-Seidel relaxation and one cell for Jacobi relaxation. The matrix equation  $(A^{2h} - B^{2h})\underline{e}^{2h} = \underline{f}^{2h}$  for red-black Gauss-Seidel relaxation case is given by

$$(16) \quad \begin{bmatrix} F & U + L \\ L + U & F \end{bmatrix} \underline{e}^{2h} = \underline{f}^{2h},$$

where  $F$ ,  $U$ , and  $L$  are the same as before with  $h$  replaced by  $2h$ . The order of variables is also the same, but for two cells instead of four cells. For Jacobi relaxation, we have

$$(17) \quad (F + U + L) \underline{e}^{2h} = \underline{f}^{2h}.$$

3. Interpolation and restriction operators. We can obtain interpolation and restriction operators in edge-edge notation from their counterparts in center-edge notation, which are given in [4], through the transformation given by equation (7). Let

$$Q_1 = \begin{bmatrix} I & 0 & 0 & 0 \\ 0 & 2I & 0 & -I \\ -I & 0 & 2I & 0 \\ 0 & 0 & 0 & I \end{bmatrix}, \quad Q = \begin{bmatrix} Q_1 & \\ & Q_1 \end{bmatrix},$$

where  $Q_1$  is the matrix for transformation (7). Denote by  $I_{2h}^{h(e)}$  and  $I_h^{2h(e)}$  the interpolation and restriction operators in the edge-edge notation, respectively, and by  $I_{2h}^{h(c)}$  and  $I_h^{2h(c)}$  the interpolation and restriction operators in the center-edge notation, respectively. It can be shown that

(18)

$$I_h^{2h(e)} = 2QI_h^{2h(c)}Q^{-1} = \begin{bmatrix} S_1 & S_2 & & \\ & & S_1 & S_2 \end{bmatrix} \quad \text{and} \quad I_{2h}^{h(e)} = QI_{2h}^{h(c)}Q^{-1} = \begin{bmatrix} T_1 & & \\ T_2 & & \\ & T_1 & \\ & & T_2 \end{bmatrix},$$

where

$$S_1 = \begin{bmatrix} 2I & 0 & 0 & 0 \\ 0 & I & 0 & 0 \\ -I & 0 & I & 0 \\ 0 & 0 & 0 & 0 \end{bmatrix}, \quad S_2 = \begin{bmatrix} 0 & 0 & 0 & 0 \\ 0 & I & 0 & -I \\ 0 & 0 & I & 0 \\ 0 & 0 & 0 & 2I \end{bmatrix},$$

$$T_1 = \begin{bmatrix} I & 0 & 0 & 0 \\ 0 & I & 0 & 0 \\ \frac{1}{2}I & 0 & \frac{1}{2}I & 0 \\ 0 & \frac{1}{2}I & 0 & \frac{1}{2}I \end{bmatrix}, \quad T_2 = \begin{bmatrix} \frac{1}{2}I & 0 & \frac{1}{2}I & 0 \\ 0 & \frac{1}{2}I & 0 & \frac{1}{2}I \\ 0 & 0 & I & 0 \\ 0 & 0 & 0 & I \end{bmatrix}.$$

#### 4. NUMERICAL EXPERIMENTS AND RESULTS

For each  $\lambda$  we have a different matrix  $Z$ . The convergence factors for the Fourier analysis are obtained as the maximum over  $\lambda(\lambda_k = \frac{\pi k}{2hP}, k = 0, \dots, P-1)$  of the spectral radius of  $Z$  (13). For a specific  $\sigma_t h$ , we evaluate the spectral radius of  $Z$  for  $P$  different frequencies ( $\lambda_k, k = 1, \dots, P-1$ ), and the convergence factor estimate from the Fourier analysis is the maximum spectral radius found. We compared the convergence factors between the Fourier analysis prediction and the convergence factor (CF) numerical results, and found a good agreement (Tables 1 and 2). In fact, for this problem the Fourier analysis prediction was

TABLE 1. Actual convergence factors (CF) and the Fourier analysis (FA) predictions for Jacobi relaxation for various values of  $\sigma_t h$  ( $S_4$  case).

$\sigma_t h$	$10^{-5}$	$10^{-4}$	$10^{-3}$	$10^{-2}$	$10^{-1}$	1.	$10^1$	$10^2$
FA	5.3E-13	2.4E-10	2.3E-7	1.3E-4	7.2E-3	5.1E-3	3.8E-5	3.5E-7
CF	9.4E-10	8.7E-7	4.1E-4	1.0E-2	1.5E-2	4.2E-3	3.9E-5	3.4E-7

more accurate than the alternative matrix analysis of convergence shown in [4].

Note that the prediction for convergence factor behaves as  $O((\frac{1}{\sigma_t h})^2)$  when  $\sigma_t h \gg 1$  and  $O((\sigma_t h)^3)$  when  $\sigma_t h \ll 1$  for both kinds of relaxation (Tables 1 and 2). This is exactly what happens with the numerical behavior. The analytical proof of convergence shown in [4] showed the convergence factor to be bounded by  $O((\frac{1}{\sigma_t h}))$  when  $\sigma_t h \gg 1$  and  $O((\sigma_t h)^2)$

TABLE 2. Actual convergence factors (CF) and the Fourier analysis (FA) predictions for red-black Gauss-Seidel relaxation for various values of  $\sigma_t h$  ( $S_4$  case).

$\sigma_t h$	$10^{-5}$	$10^{-4}$	$10^{-3}$	$10^{-2}$	$10^{-1}$	1.	$10^1$	$10^2$
FA	3.5E-13	1.2E-10	1.2E-7	8.7E-5	3.8E-3	8.2E-4	3.2E-5	2.7E-7
CF	3.3E-10	2.8E-7	7.2E-5	4.3E-3	8.0E-3	1.1E-3	3.17E-5	2.5E-7

when  $\sigma_t h \ll 1$  for both kinds of relaxation. The analytical results shown here confirm that the analytical bounds were not sharp. From the results shown in Tables 1 and 2 we notice that the FA results are in fact smaller than the actual numerical CF from the real multigrid codes; this is because the Fourier analysis described here uses a two grid approach. The usefulness of Fourier Analysis is due to the fact that it explains the behavior of the actual multigrid algorithm without the hard work of implementing it.

#### REFERENCES

1. E. W. Larsen. Unconditionally stable diffusion-synthetic acceleration methods for the slab geometry discrete ordinates equations. *Nucl. Sci. Eng.*, 82:47–63, 1982.
2. E. W. Larsen and J. E. Morel. Asymptotic solutions of numerical transport problems in optically thick, diffusive regimes II. *J. Comput. Phys.*, 83:212–236, 1989.
3. T. A. Manteuffel, S. F. McCormick, J. Morel, S. Oliveira, and G. Yang. A parallel version of a multigrid algorithm for isotropic transport equations. *SIAM J. Sci. Comput.*, 15:474–493, March 1994.
4. T. A. Manteuffel, S. F. McCormick, J. Morel, S. Oliveira, and G. Yang. A fast multigrid algorithm for isotropic transport problems. I. Pure scattering. *SIAM J. Sci. Comput.*, 16:601–635, May 1995.
5. J. E. Morel and T. A. Manteuffel. An angular multigrid acceleration technique for the  $S_n$  equations with highly forward-peaked scattering. *Nucl. Sci. Eng.*, 107:330–342, 1991.
6. S. Oliveira. A parallel multilevel algorithm for anisotropic transport equations. *Computational Techniques and Applications: CTAC93, World Scientific Publ.*, pages 388–396, 1994.
7. S. Oliveira. Krylov subspace methods for transport equations. *10th ENFIR Meeting on Reactor Physics*, pages 523–528, August 1995.
8. S. Oliveira. Multigrid and Krylov subspace methods for transport equations: Absorption case. *Proceedings of the 7th Copper Mountain Conference on Multigrid Methods, NASA Conference Publications*, pages 637–648, 1996.
9. S. Oliveira. Parallel multigrid methods for transport equations: the anisotropic case. *Parallel Computing*, 22:513–537, 1996.
10. S. Oliveira and Y. Deng. Preconditioned Krylov subspace methods for transport equations. *Progress in Nuclear Energy*, 1997. To appear.
11. P. Wesseling. *An Introduction to Multigrid Methods*. John Wiley & Sons, Chichester, 1992.